COMPUTER SIMULATIONS OF DORSAL COCHLEAR NUCLEUS NEURAL CIRCUITRY

K.E. Hancock[1], K.A. Davis[2], and H.F. Voigt[3]
[1]Eaton-Peabody Laboratory, Massachusetts Eye & Ear Infirmary, Boston, MA, USA
[2]Departments of Biomedical Engineering and Neurobiology & Anatomy, University of Rochester, Rochester, NY, USA
[3]Hearing Research Center and Department of Biomedical Engineering, Boston University, Boston, MA, USA

Abstract – **The dorsal cochlear nucleus (DCN) is part of the first stage of auditory processing in the central nervous system. Experimental evidence has provided a conceptual model for a portion of the DCN neural circuit that serves as a basis for the computational model described in this paper.**

The model consists of four neural populations arranged tonotopically. The pattern of convergence from one population to another and the strengths of those connections are important model parameters. Lumped parameter electrical circuit models are used to model the membrane potential of individual cells. Synapses are simulated by activating variable conductances in postsynaptic cells according to spike activity in presynaptic cells. The level of detail incorporated in the model is a good compromise between biophysical accuracy and the computational tractability required to simulate relatively large networks.

Results are shown demonstrating the ability of the model to replicate features of DCN cross-correlation functions and to simulate DCN response properties with quantitative accuracy. The model is a useful tool for exploring hypotheses regarding DCN structure and function.

Keywords - **cochlear nucleus, hearing, computational modeling, parameter estimation**

I. INTRODUCTION

The most well understood component of the dorsal cochlear nucleus (DCN) neural circuit centers around the interaction of type II and type IV units. Type II units are characterized by a lack of spontaneous activity and a weak response to broadband noise [1]. Their responses to best frequency (BF) tones feature large firing rates that increase with sound pressure level up to a point beyond which firing rates gradually decrease. Type IV units are spontaneously active and generally excited by broadband noise. They are excited by BF tones for levels near threshold, but strongly inhibited at higher levels [2]. Type IV units have been associated with the projection neurons of the DCN [3]. The reciprocal nature of the response properties of type II units and type IV units led to a conceptual model of the DCN in which both unit types receive excitatory input from the auditory nerve (AN) while type II units inhibit type IV units [4]. Further evidence for an inhibitory interaction between type II and type IV units was later provided by cross-correlation experiments [5, 6].

Experiments using notch noise stimuli have suggested another important source of inhibition onto type IV units [7, 8]. Type IV units give excitatory responses to noise containing very narrow notches. Responses decrease with increasing notch width, eventually becoming inhibitory. For the widest notches, the response approaches the spontaneous rate of the unit. Such behavior is consistent with the existence of a broadly-tuned source of inhibition, or wideband inhibitor (WBI) [7]. The WBI is presumed to be less sensitive than type IV units to the missing energy in the notch, so that as the notch is widened, the balance of synaptic drive to the type IV unit shifts from excitatory to inhibitory. The WBI may also be responsible for suppressing the responses of type II units to broadband noise.

This paper describes a computational model of DCN neural circuitry based on the interactions of AN fibers, type II units, type IV units and the WBI. Simulations are shown dealing with the interactions of DCN units in response to tonal stimuli, and DCN responses to wideband stimuli. All results are drawn from our previous modeling studies [9-13].

II. METHODOLOGY

A. Organization of the model

The model consists of 800 isofrequency slices, each containing a single AN fiber, as shown in Fig. 1A. AN fibers were simulated using the model of Carney [15] and were assigned characteristic frequencies from 1.25 kHz to 10 kHz in 0.005 octave steps. The model thus spans 4 octaves and is centered at 5 kHz.

A nomenclature for naming model elements was developed in order to distinguish clearly model results from experimental results. Thus, in addition to an AN fiber, each slice contains one W-cell (model WBI), one I2-cell (model type II unit) and one P-cell (principal cell, model type IV unit). The source labeled “nonspecific afferents” provides tonic excitatory drive to the P-cells.

The model populations were connected in a manner consistent with the conceptual model of DCN neural circuitry (Fig. 1A). Three parameters were used to specify the convergence of one population onto another, as illustrated in Fig. 1B for two populations labeled “A” and “B”. Each target cell in “B” receives input from $N_{A\rightarrow B}$ source cells “A”, drawn randomly from a band $BW_{A\rightarrow B}$ octaves wide. The octave ratio of the source band center frequency to the target cell best frequency is indicated by the parameter $C_{A\rightarrow B}$.

B. Single cell model

Individual W-, I2-, and P-cells were implemented using the

This work was supported by the Whitaker Foundation and NIDCD.

Report Documentation Page

Report Date	Report Type	Dates Covered (from... to)
25 Oct 2001	N/A	-

Title and Subtitle Computer Simulations of Dorsal Cochlear Nucleus Neural Circuitry	**Contract Number**
	Grant Number
	Program Element Number
Author(s)	**Project Number**
	Task Number
	Work Unit Number
Performing Organization Name(s) and Address(es) Eaton-Peabody Laboratory Massachusetts Eye & Ear Infirmary Boston, MA	**Performing Organization Report Number**
Sponsoring/Monitoring Agency Name(s) and Address(es) US Army Research, Development & Standardization Group (UK) PSC 803 Box 15 FPO AE 09499-1500	**Sponsor/Monitor's Acronym(s)**
	Sponsor/Monitor's Report Number(s)

Distribution/Availability Statement
Approved for public release, distribution unlimited

Supplementary Notes
Papers from 23rd Annual International Conference of the IEEE Engineering in Medicine and Biology Society, October 25-28, 2001, held in Istanbul, Turkey. See also ADM001351 for entire conference on cd-rom.

Abstract

Subject Terms

Report Classification unclassified	**Classification of this page** unclassified
Classification of Abstract unclassified	**Limitation of Abstract** UU

Number of Pages
4

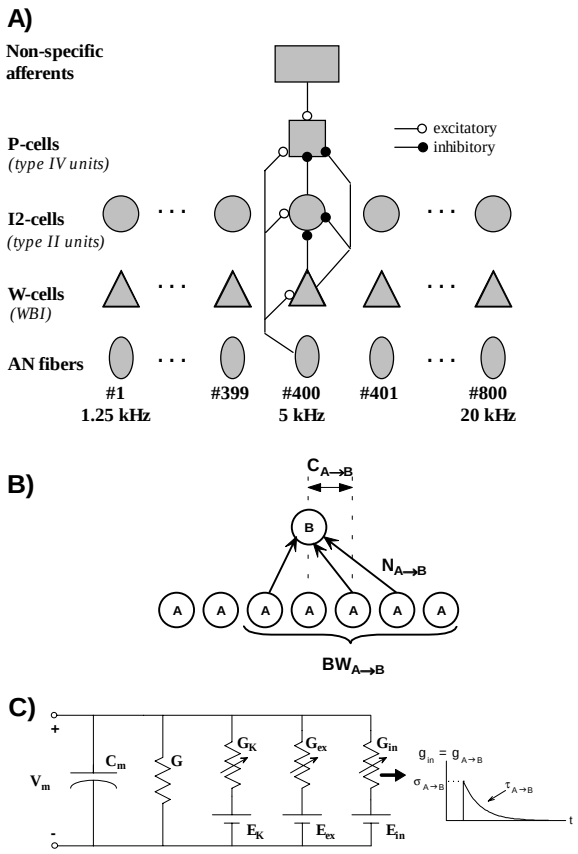

Fig. 1. (A) Diagram illustrating the connections between the cell populations of the DCN model. The populations are arranged in a tonotopic fashion. (B) Parameters used to specify the convergence of a cell population "A" onto a target cell from population "B". (C) Lumped parameter electric circuit model used to model the membrane potential of single cells. C_m, membrane capacitance; G, resting conductance; G_K, G_{ex}, G_{in}, variable potassium, excitatory synaptic and inhibitory synaptic conductances, respectively; E_K, E_{ex}, E_{in}, corresponding reversal potentials. Synaptic activation results in the conductance change shown. Modified from [13].

neuromime of MacGregor [14], shown in Fig. 1C. Two branches represent the membrane capacitance and leakage conductance, specified jointly by the membrane time constant τ_m. Synapses are effected by means of variable conductances such as those illustrated in the two rightmost branches of Fig. 1C. Each model neuron has one such branch for each population from which it receives input. An action potential in a source cell "A" activates the conductance $g_{A\to B}$ in a target cell "B". The activation consists of a step increase and exponential decay where the step size $\sigma_{A\to B}$ and time constant $\tau_{A\to B}$ are important model parameters. Note that the sign of the synapse is determined by the value of the associated reversal potential.

Voltage dependent conductances underlying the action potential were not simulated. Rather, when the membrane potential exceeded its threshold θ, the event time was recorded and the variable potassium conductance underwent a step increase of height b_K followed by an exponential decay with time constant τ_K.

III. Results

A. Cross-correlation simulations

The model was used to explore mechanisms underlying certain stimulus-dependent effects that have been observed in experimentally obtained cross-correlograms [9-11]. For example, Fig. 2A shows the cross-correlation of spike trains from one I2-cell and one P-cell at three different sound pressure levels. The correlograms are derived from responses to 50-s BF tones and are referenced to the I2-cell spike train. The primary feature is an inhibitory trough (IT) that represents a decrease in P-cell discharge probability following an I2-cell event and is consistent with the known inhibitory connection between these two model cells. Note that the IT decreases in size as a function of stimulus level. The simulated ITs of Fig. 2A are qualitatively similar to those obtained experimentally from type II-type IV unit pairs [5, 6].

"Effectiveness" is a measure of IT strength computed by finding the area of the cross-correlogram beneath the mean discharge rate (black filled regions in Fig. 2A). Fig. 2B plots effectiveness as a function of stimulus level for model (symbols) and experimental (bold lines) data. The model successfully replicates the experimentally observed decrease in effectiveness with increasing stimulus level. Furthermore, since the I2-cell to P-cell synapse is constructed to be nonmodifiable, the level dependency is due to the overall decrease in P-cell discharge rate, rather than plasticity in the circuit [11]. Finally, effectiveness values tend to be larger for the simulations than for the experimental data. It was possible to shift the model effectiveness curves by trading an increase in the parameter $N_{I2\to P}$ for a decrease in $\sigma_{I2\to P}$ [11]. In this way, the cross-correlation data provided a basis for constraining the connection parameters of the model.

B. Simulations of type II units

Accurate simulations of type II units were made possible by the addition of wideband inhibition to the model. Fig. 3A shows the rate-level curves for a representative I2-cell in response to BF tones and broadband noise. The weak noise response, and vigorous but nonmonotonic BF tone response are characteristic of DCN type II units.

The parameter $BW_{AN\to W}$ was optimized by systematically varying its value over a range of 4 octaves (Fig. 3B). At each step, the product of $N_{AN\to W}$ and $\sigma_{AN\to W}$ was adjusted to give a weak noise response (~25 spike/s). The falling slope of the I2-cell BF tone rate-level curve was then plotted as a function of $BW_{AN\to W}$. Most type II units have normalized tone slopes greater than –0.012/dB. This was achieved by the model when $BW_{AN\to W}$ was at least 2.8 octaves. Interestingly, experimental evidence suggests that the putative source of

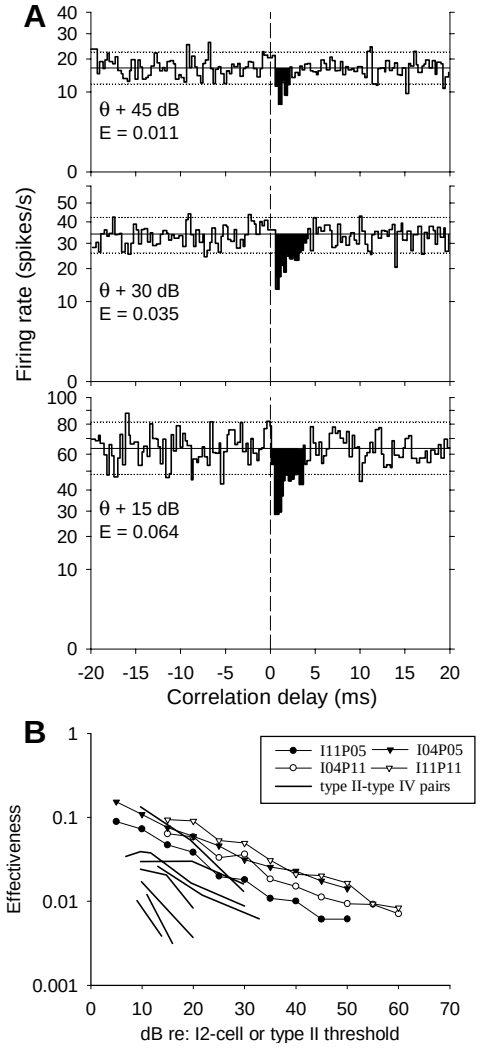

Fig. 2. (A) Cross-correlograms derived from spike trains of one I2-cell and one P-cell, at three different levels. The I2-cell provides one inhibitory synapse to the P-cell and is the reference unit. Center line indicates mean discharge rate. Dotted lines indicate the ±2 standard deviation confidence limits expected for independent firing. Binwidth = 0.3ms. E, effectiveness; θ, I2-cell threshold (~10 dB SPL). (B) Plots of effective versus sound pressure level for four model I2-cell/P-cell pairs and eight type II-type IV unit pairs. Level is plotted with respect to either the I2-cell or type II unit threshold. Modified from [11].

wideband inhibition to the DCN has a bandwidth of about 3 octaves [16].

C. Wideband inhibition of type IV units

The incorporation of wideband inhibition also made possible quantitatively accurate simulations of type IV unit notch noise responses (Fig. 4). Qualitative results suggested that the parameters $BW_{AN\rightarrow W}$, $\sigma_{AN\rightarrow P}$, and $\sigma_{W\rightarrow P}$ determine the major features of the rate-versus-cutoff-frequency plots. These parameters were then systematically varied to produce 900 simulated data sets. A brute force search was used to find the parameter set that minimized the sum of the squared error (SSE) between data and model. Fig. 4A shows one example of a good model fit to the notch noise response of a DCN type IV unit.

The sensitivity of the fit to the parameter values is illustrated by the contours of equal SSE in Fig. 4B-D. In each panel, a different parameter is held fixed at its optimal value. The contours tend to be elliptical in shape and suggest that the objective function has a compact minimum. This indicates that the fit is indeed sensitive to the parameter values and that the optimal fit is relatively unique.

IV. Discussion

This model represents a balance between biophysical accuracy at the single cell level and the computational tractability of simulating a relatively large neural network. The MacGregor neuromime is computationally efficient because it omits the details of the Hodgkin-Huxley conductances as well as the complexities of dendritic cable properties. At the same time, it provides a rudimentary representation of synaptic physiology and the integrative properties of a cell membrane. Purely algebraic network models might simulate the steady state behavior of DCN neurons with reasonable accuracy and great speed, but lack the temporal structure necessary to investigate time-dependent phenomenon, such as the cross-correlation results of Fig. 2. Thus, we feel the implementation described here provides greater flexibility in terms of the range of physiological data that can be explored.

A quantitative approach proved useful in optimizing parameter values and assessing simulation accuracy, as illustrated in Figs. 3-4. Sensitivity analysis was particularly useful for quantifying the uniqueness of optimal parameter fits. Given that type IV units arise from both fusiform and giant cells of the DCN, it may be possible for the parameter estimation techniques described here to provide a basis for segregating physiological data according to anatomical substrate.

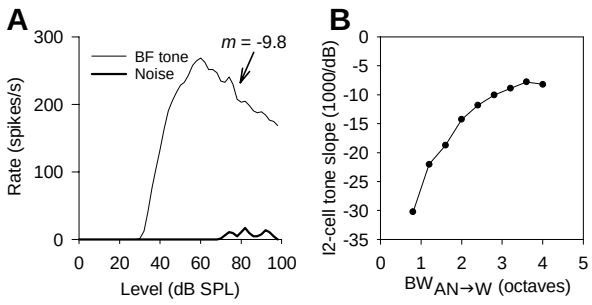

Fig. 3. (A) I2-cell rate-level curves are similar to those of DCN type II units. *m*, normalized tone slope (1000/dB) which is the slope of the falling portion of the BF rate-level curve normalized by the maximum firing rate. (B) Normalized tone slope as a function of W-cell bandwidth. Modified from [12].

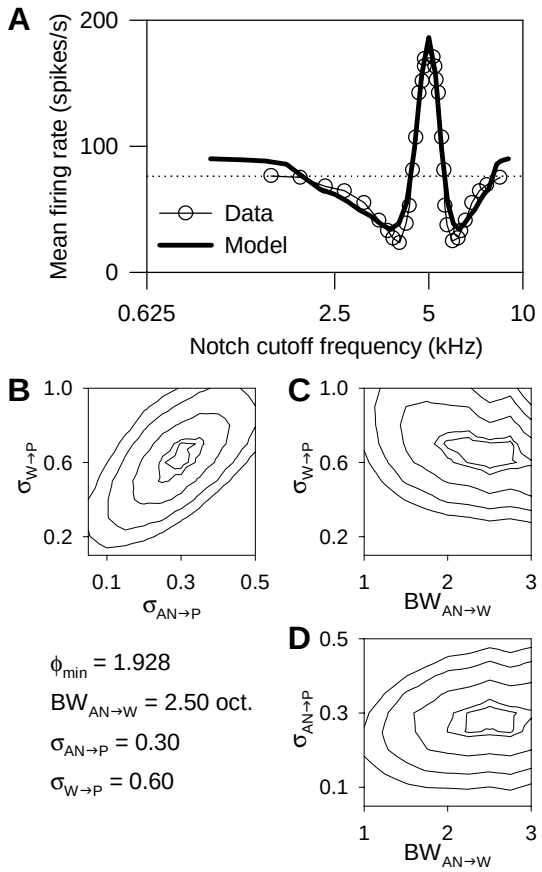

Fig. 4. (A) Best fit of the model to type IV unit notch noise response data. Fit was obtained by minimizing the SSE over the three parameters $BW_{AN\to W}$, $\sigma_{AN\to P}$, and $\sigma_{W\to P}$. (B-D) Equal SSE contours demonstrating the sensitivity of the fit to parameter values. The contours represent SSE/SSE_{min} = 1.5, 2, 5, 10, and 15 from inside to outside. In each panel, a different parameter is held fixed at its optimal value. Data from [8]. Figure modified from [13].

V. Conclusion

This paper has highlighted the ability of our model to replicate features of DCN cross-correlation functions and to simulate type II unit and type IV unit responses with quantitative accuracy. Other studies have used the model to explore differences in DCN physiology between cats and gerbils [10] and to investigate the effects of barbiturate anesthesia on DCN response patterns [17]. The model has thus proven to be a useful tool for exploring hypotheses regarding DCN structure and function.

References

[1] E. D. Young and H. F. Voigt, "Response properties of type II and type III units in dorsal cochlear nucleus," *Hearing Research*, vol. 6, pp. 153-169, 1982.

[2] E. F. Evans and P. G. Nelson, "The responses of single neurons in the cochlear nucleus of the cat as a function of their location and the anesthetic state," *Exp. Brain Res.*, vol. 17, pp. 402-427, 1973.

[3] E. D. Young, "Identification of response properties of ascending axons from dorsal cochlear nucleus," *Brain Research*, vol. 200, pp. 23-38, 1980.

[4] E. D. Young and W. E. Brownell, "Responses to tones and noise of single cells in dorsal cochlear nucleus of unanesthetized cats," *J. Neurophysiol.*, vol. 39, pp. 282-300, 1976.

[5] H. F. Voigt and E. D. Young, "Evidence of inhibitory interactions between neurons in the dorsal cochlear nucleus," *J. Neurophysiol.*, vol. 44, pp. 76-96, 1980.

[6] H. F. Voigt and E. D. Young, "Neural cross-correlation analysis of inhibitory interactions in dorsal cochlear nucleus," *J. Neurophysiol.*, vol. 64, pp. 1590-1610, 1990.

[7] I. Nelken and E. D. Young, "Two separate inhibitory mechanisms shape the responses of dorsal cochlear nucleus type IV units to narrowband and wideband stimuli," *J. Neurophysiol.*, vol. 71, pp. 2446-2462, 1994.

[8] G. A. Spirou and E. D. Young, "Organization of dorsal cochlear nucleus type IV unit response maps and their relationship to activation by band-limited noise," *J Neurophysiol*, vol. 66, pp. 1750-1768, 1991.

[9] K. A. Davis and H. F. Voigt, "Neural modeling of the dorsal cochlear nucleus: cross-correlation analysis of short-duration tone-burst responses," *Biol Cybern*, vol. 71, pp. 511-521, 1994.

[10] K. A. Davis and H. F. Voigt, "Computer simulation of shared input among projection neurons in the dorsal cochlear nucleus," *Biol Cybern*, vol. 74, pp. 413-425, 1996.

[11] H. F. Voigt and K. A. Davis, "Computer simulations of neural correlations in the dorsal cochlear nucleus.," in *Cochlear Nucleus: Structure and Function in Relation to Modeling*, W. A. Ainsworth, Ed. London: JAI Press, 1996, pp. 351-375.

[12] K. E. Hancock, K. A. Davis, and H. F. Voigt, "Modeling inhibition of type II units in the dorsal cochlear nucleus," *Biol. Cybern.*, vol. 76, pp. 419-428, 1997.

[13] K. E. Hancock and H. F. Voigt, "Wideband inhibition of dorsal cochlear nucleus type IV units in cat: a computational model," *Ann Biomed Eng*, vol. 27, pp. 73-87, 1999.

[14] R. J. MacGregor, *Neural and Brain Modeling*. San Diego: Academic Press, 1987.

[15] L. H. Carney, "A model for the responses of low-frequency auditory nerve fibers in cat," *J Acoust Soc Am*, vol. 93, pp. 401-417, 1993.

[16] A. R. Palmer, D. Jiang, and D. H. Marshall, "Responses of ventral cochlear nucleus onset and chopper units as a function of signal bandwidth," *J. Neurophysiol.*, vol. 75, pp. 780-794, 1996.

[17] H. Fan, "The Effects of Barbiturates on the Response Properties of Dorsal Cochlear Nucleus (DCN) Neurons in Decerebrate Gerbil". Boston, MA: Boston University, 2000.